

A Very Narrow Shadow Extra Z-boson at Colliders

We-Fu Chang,^{1,*} John N. Ng,^{2,†} and Jackson M. S. Wu^{2,‡}

¹*Institute of Physics, Academia Sinica, Nankang, Taipei, Taiwan 115*

²*Theory group, TRIUMF, 4004 Wesbrook Mall, Vancouver, B.C., Canada*

(Dated: October 10, 2018)

We consider the phenomenological consequences of a hidden Higgs sector extending the Standard Model (SM), in which the “shadow Higgs” are uncharged under the SM gauge groups. We consider a simple $U(1)$ model with one Higgs singlet. One mechanism which sheds light on the shadow sector is the mixing between the neutral gauge boson of the SM and the additional $U(1)$ gauge group. The mixing happens through the usual mass-mixing and also kinetic-mixing, and is the only way the “shadow Z ” couples to the SM. We study in detail modifications to the electroweak precision tests (EWPTs) that the presence of such a shadow sector would bring, which in turn provide constraints on the kinetic-mixing parameter, s_ϵ , left free in our model. The shadow Z production rate at the LHC and ILC depends on s_ϵ . We find that observable event rate at both facilities is possible for a reasonable range of s_ϵ allowed by EWPTs.

I. INTRODUCTION

In the pursuit of physics beyond the Standard Model (SM) it is very common to encounter one or more Abelian gauge symmetry than the SM $U(1)$ hypercharge. Two familiar examples are the grand Unified theories (GUTs) based on $SO(10)$ that breaks to $G_{SM} \times U(1)$, where G_{SM} is the SM gauge group and $E(6)$ which ultimately breaks to $G_{SM} \times U(1) \times U(1)$. Because of their GUTs parentage the extra Z bosons from the breaking of the $U(1)$ symmetries have tree level couplings to the SM particles; in particular the fermions. This makes them highly visible and their phenomenology has been well studied [1]. More recently extra dimensional models with extra $U(1)$ gauge symmetries in the brane world scenario are increasingly popular. A feature of this newer construction is that the extra $U(1)$ factors can be hidden from the visible sector. Hidden sectors are motivated also by studies in supersymmetry breaking mechanisms. Independent of the theoretical motivation, extra Z bosons from hidden sector typically do not have direct couplings to the SM particles. Their phenomenology can be very different from visible extra Z 's. They are also harder to produce. As the start up of the LHC draws near, the search for extra Z bosons is a high priority item due to their relatively clean signatures from Drell-Yan processes. Clearly it is important to include hard to find extra Z bosons in this search. Although these bosons have no direct couplings to SM particles, they can manifest themselves through mixings with the SM Z boson, and so are not completely invisible. Since the mixing is crucial for phenomenology we construct the simplest model of this kind to capture the physics of such an extra Z boson. It has the gauge symmetry $G_{SM} \times U(1)_s$ where the subscript denotes “shadow”; the name will become clear later. The

SM fermions are singlet under $U(1)_s$. This $U(1)_s$ is broken by a shadow Higgs sector which is just the Abelian Higgs model with a complex scalar ϕ_s . The ϕ_s field is a singlet under G_{SM} but interacts with the SM Higgs bosons via renormalizable interactions. The complete Lagrangian is given by

$$\mathcal{L} = \mathcal{L}_{SM} - \frac{1}{4} X^{\mu\nu} X_{\mu\nu} - \frac{\epsilon}{2} B^{\mu\nu} X_{\mu\nu} + \left| \left(\partial_\mu - \frac{1}{2} g_s X_\mu \right) \phi_s \right|^2 - V(\phi_s, \Phi), \quad (1)$$

where $B_{\mu\nu}$ is the field strength tensor of the SM hypercharge $U(1)_Y$, Φ is the SM Higgs field, and g_s is the gauge coupling of the shadow $U(1)_s$. For simplicity we have normalized the shadow charge of ϕ_s to unity. The kinematic mixing of the two $U(1)$'s is parameterized by ϵ , which a priori need not be a small number. For a visible extra Z this mixing term is expected to be only induced at the loop level [2], and thus $|\epsilon| \ll 1$ is generally assumed in its phenomenological studies [3]. However, this need not be the case here. Indeed, a calculation in string theory of the mixing-generating vacuum polarization diagram shows that in general, one can expect kinetic mixing effects on the order of $10^{-4} \sim 10^{-2}$ at the weak scale (barring accidental cancellations in the tree level spectrum) [4]. Given the theoretical significance outlined above, we shall leave ϵ as a free parameter to be constrained by experiments in particular the electroweak precision tests (EWPTs). Now it is well known that the kinetic terms including the mixing can be recast into canonical form through a $GL(2)$ transformation. Explicitly, this is given by

$$\begin{pmatrix} X \\ B \end{pmatrix} = \begin{pmatrix} c_\epsilon & 0 \\ -s_\epsilon & 1 \end{pmatrix} \begin{pmatrix} X' \\ B' \end{pmatrix}, \quad (2)$$

where

$$s_\epsilon = \frac{\epsilon}{\sqrt{1-\epsilon^2}}, \quad c_\epsilon = \frac{1}{\sqrt{1-\epsilon^2}}. \quad (3)$$

After spontaneous symmetry breaking (SSB) X' and B' will mix resulting in a shift in the SM Z mass. The

*Electronic address: wfchang@phys.sinica.edu.tw

†Electronic address: misery@triumf.ca

‡Electronic address: jwu@triumf.ca

physical bosons are now linear combinations of the two. The photon will remain massless, and the W bosons will be unchanged from the SM. This is expected since the shadow sector only interacts with $U(1)_Y$ through the shadow Higgs interactions. The details of this symmetry breaking is given in Sec. II. Feynman rules for the model are also given there. In this paper we focus on the phenomenology of the physical shadow sector neutral boson, Z_s . Since we are interested in collider physics we shall assume that vacuum expectation value (VEV) of ϕ_s is of the order of the weak scale or higher. In Sec. III we study the impact Z_s has on electroweak precision measurements. From these, as well as anomalous magnetic moment of the muon and recent results from Møller scattering, we derive constraints on the parameters of our model, in particular on s_ϵ . We employ a conservative strategy and demand that the fits to the data are not much worse than that of the SM. With these limits in hand we explore the prospect of observing the Z_s at the LHC and the ILC in Sec. IV. Finally we give our conclusions in Sec. V. Recent work with an extra Z similar to ours is given in [5] and the older literature can be found in [6, 7].

II. SYMMETRY BREAKING AND THE SHADOW WORLD

The most general renormalizable $G_{SM} \times U(1)_s$ invariant scalar potential is:

$$V(\Phi, \phi_p) = \mu_s^2 \phi_s^* \phi_s + \lambda_s (\phi_s^* \phi_s)^2 + 2\kappa (\Phi^\dagger \Phi) (\phi_s^* \phi_s) + \mu^2 \Phi^\dagger \Phi + \lambda (\Phi^\dagger \Phi)^2. \quad (4)$$

This Higgs potential is also used in phantom Higgs models [8]. After SSB the scalars acquire nonzero VEV,

$$\langle \Phi \rangle = \frac{1}{\sqrt{2}} \begin{pmatrix} 0 \\ v_0 \end{pmatrix}, \quad \langle \phi_p \rangle = \frac{v_s}{\sqrt{2}}, \quad (5)$$

with

$$v_0^2 = -\frac{\lambda_s \mu^2 - \kappa \mu_s^2}{\lambda \lambda_s - \kappa^2}, \quad v_s^2 = -\frac{\lambda \mu_s^2 - \kappa \mu^2}{\lambda \lambda_s - \kappa^2}. \quad (6)$$

To ensure that the potential is bounded from below and the above values correspond to a global minimum we require $\lambda, \lambda_s > 0$ and $\kappa > 0$.

The $SU(2)_L \times U(1)_Y \times U(1)_s$ symmetry is broken down to $U(1)_{QED}$. This pattern of breaking is peculiar in that the mass of the W boson remains as in the SM, i.e. $M_W = (g_2 v_0)/2$. In the neutral sector we have a massless photon and two massive neutral bosons which are not yet in the mass eigenbasis. The usual SM definition: $\tan \theta_W = g_Y/g_2$, electric charge $e = g_2 \sin \theta_W$, and $Q_{L,R}^f = T_{L,R}^3 + Y_{L,R}^f$ remain intact.

For the neutral gauge bosons the transformation between the weak and mass basis is given by the following

rotation:

$$\begin{pmatrix} B' \\ A_3 \\ X' \end{pmatrix} = \begin{pmatrix} c_W & -s_W & 0 \\ s_W & c_W & 0 \\ 0 & 0 & 1 \end{pmatrix} \begin{pmatrix} 1 & 0 & 0 \\ 0 & c_\eta & -s_\eta \\ 0 & s_\eta & c_\eta \end{pmatrix} \begin{pmatrix} \gamma \\ Z \\ Z_s \end{pmatrix}, \quad (7)$$

where s_W (c_W) denotes $\sin \theta_W$ ($\cos \theta_W$) and similarly for the rotation angle η . The first rotation is the standard one that gives rise to the SM Z and the second one diagonalizes the mixing of the two Z bosons. The mixing angle is given by

$$\tan 2\eta = \frac{2s_W s_\epsilon}{c_W^2 (M_3/M_W)^2 + s_W^2 s_\epsilon^2 - 1}, \quad (8)$$

where $M_3 \equiv (g_s v_s)/2$. For small s_ϵ and $c_W M_3 > M_W$, $\eta < \epsilon$. The masses for the two massive neutral gauge bosons are readily found to be

$$M_{Z, Z_s}^2 = \frac{M_W^2}{2c_W^2} \left\{ \left(\frac{c_W M_3}{M_W} \right)^2 + 1 + s_W^2 s_\epsilon^2 \mp \sqrt{[(c_W M_3/M_W)^2 - 1 + s_W^2 s_\epsilon^2]^2 + 4s_W^2 s_\epsilon^2} \right\}, \quad (9)$$

For the case where $M_3 > M_W$ the Z - Z_s mixing is proportional to s_ϵ , which is related to the amplitude of the kinetic mixing term $B^{\mu\nu} X_{\mu\nu}$.

The most stringent constraints on any extra Z model come from EWPTs, and so we consider next the gauge fermion couplings. These can be readily read off from the Lagrangian. For the photon (A^μ), the SM result is retained as it should:

$$A^\mu \bar{f} f : i\gamma^\mu e Q_f. \quad (10)$$

For Z, Z_s , the coupling are slightly different from the SM, but still flavor universal:

$$Z^\mu \bar{f} f : i\gamma^\mu \frac{g_2}{c_W} \left[(c_\eta g_f^L - s_\eta s_W s_\epsilon Y_f^L) \hat{L} + (c_\eta g_f^R - s_\eta s_W s_\epsilon Y_f^R) \hat{R} \right], \quad (11)$$

$$Z_s^\mu \bar{f} f : i\gamma^\mu \frac{g_2}{c_W} \left[(-s_\eta g_f^L - c_\eta s_W s_\epsilon Y_f^L) \hat{L} + (-s_\eta g_f^R - c_\eta s_W s_\epsilon Y_f^R) \hat{R} \right], \quad (12)$$

where $g_{L,R}^f = T^3(f_{L,R}) - s_W^2 Q^f$ is the coupling of the SM Z to fermions. We see that the neutral current couplings are not only rotated as indicated by the c_η factor, but also contain an extra piece proportional to the fermion hypercharge due to $U(1)$ - $U(1)_s$ mixing. Hence we need to reexamine the electroweak precision data using the full couplings as well as taking into account the effects due to virtual Z_s exchanges. For the pure gauge sector, it's straightforward to work out the Feynman rules. For example, the Feynman rules for 4 gauge boson ($V_\mu^1 V_\nu^2 W_\lambda^+ W_\rho^-$) vertex read:

$$-i g_2^2 C_4^{V_1, V_2} [2g_{\mu\nu} g_{\lambda\rho} - g_{\mu\lambda} g_{\nu\rho} - g_{\mu\rho} g_{\nu\lambda}], \quad (13)$$

where the factor C_4 are listed below:

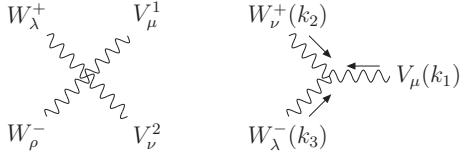


FIG. 1: The triple and quartic gauge vertices and the momentum labelling.

| | | | | | |
|--------------------|------------------|------------------|------------------|-------------------|------------------------|
| (γ, γ) | (Z, Z) | (Z_s, Z_s) | (γ, Z) | (γ, Z_s) | (Z, Z_s) |
| s_W^2 | $c_W^2 c_\eta^2$ | $c_W^2 s_\eta^2$ | $s_W c_W c_\eta$ | $-s_W c_W s_\eta$ | $-c_W^2 s_\eta c_\eta$ |

Similarly, the Feynman rules for triple gauge coupling for $V_\mu(k_1)W_\nu^+(k_2)W_\lambda^-(k_3)$, where all momentum k 's go into the vertex, read:

$$-ig_2 C_3^V [(k_1 - k_2)_\lambda g_{\mu\nu} + (k_2 - k_3)_\mu g_{\nu\lambda} + (k_3 - k_1)_\nu g_{\lambda\mu}], \quad (14)$$

and for different V s the C_3 's are

| | | |
|----------|--------------|---------------|
| γ | Z | Z_s |
| s_W | $c_W c_\eta$ | $-c_W s_\eta$ |

Now a few remarks about the scalar sector. The SM Higgs doublet has 4 degrees of freedom (DOF) and the shadow scalar has 2 DOF. After SSB in both sectors, one DOF of each scalar becomes massive physical scalar. So we are left with 3 + 1 massless DOFs which will be eaten by two W , one Z , and one Z_s , and the DOF budget is balanced. Therefore, the shadow world gives us one extra neutral scalar and no charged scalars. How heavy they are is an interesting question. We will assume here the lighter one is SM-like and has a mass greater than 114 GeV and the heavier one is more than 200 GeV. This amounts to assuming $v_s \gtrsim v_0$ and no fine tuning of the Higgs parameters. In the basis of $\{h_{SM}^0, h_s^0\}$, the mass matrix for these two neutral scalars is

$$\begin{pmatrix} \lambda v_0^2 & \kappa v_0 v_s \\ \kappa v_0 v_s & \lambda_p v_s^2 \end{pmatrix}. \quad (15)$$

It can be diagonalized by a rotation

$$\begin{pmatrix} h_{SM}^0 \\ h_s^0 \end{pmatrix} = \begin{pmatrix} \cos \alpha & \sin \alpha \\ -\sin \alpha & \cos \alpha \end{pmatrix} \begin{pmatrix} h_1^0 \\ h_2^0 \end{pmatrix}, \quad (16)$$

and the mixing angle satisfies

$$\tan(2\alpha) = \frac{2\kappa v_0 v_s}{\lambda_s v_s^2 - \lambda v_0^2}, \quad (17)$$

with mass square

$$m_{1,2}^2 = \frac{1}{2} \left[\lambda_s v_s^2 + \lambda v_0^2 \pm \sqrt{(\lambda_p v_p^2 - \lambda v_0^2)^2 + 4\kappa^2 v_s^2 v_0^2} \right]. \quad (18)$$

The Feynman rules for the scalar sector can be readily worked out. For instance, in the mass basis of the

fermions, the scalar-fermion couplings are given by

$$h_1^0 \bar{f} f : -i \cos \alpha \frac{g_2 m_f}{\sqrt{2} M_W}, \quad (19)$$

$$h_2^0 \bar{f} f : -i \sin \alpha \frac{g_2 m_f}{\sqrt{2} M_W}, \quad (20)$$

and for the gauge-scalar couplings one has

$$h_1^0 Z^\mu Z^\nu : \frac{ig_2 M_W}{c_W^2} c_\alpha (c_\eta + s_W s_\epsilon s_\eta)^2 g^{\mu\nu}, \quad (21)$$

$$h_1^0 Z_s^\mu Z_s^\nu : \frac{ig_2 M_W}{c_W^2} c_\alpha (s_\eta - s_W s_\epsilon c_\eta)^2 g^{\mu\nu}, \quad (22)$$

$$h_1^0 Z_s^\mu Z^\nu : -\frac{ig_2 M_W}{c_W^2} c_\alpha g^{\mu\nu} \times (c_\eta + s_W s_\epsilon s_\eta)(s_\eta - s_W s_\epsilon c_\eta), \quad (23)$$

$$h_1^0 W^{+\mu} W^{-\nu} : ig_2 M_W c_\alpha g^{\mu\nu}. \quad (24)$$

For h_2^0 , the ‘‘shadow Higgs’’, c_α is replaced by s_α in the above expression.

III. PHENOMENOLOGY

We now perform a systematic phenomenological study using the Feynman rules derived previously. We present the analytical result involving parameters of the shadow sector; numerical values are summarized in Table I at the end of the section. We begin with the anomalous magnetic moment of the muon.

A. Muon $g - 2$

The one-loop Z boson contribution to the anomalous magnetic moment of a charged lepton is now different from the SM due to modification of its coupling to fermions. Furthermore, the same one-loop diagram with Z_s running in the loop contributes as well. Plugging in the gauge-fermion interactions obtained in the previous section, the SM one-loop Z boson contribution now shifts by an amount:

$$\begin{aligned} \delta a_\mu &= s_\eta^2 \Delta a_Z^{SM} \left[1 - \left(\frac{M_Z}{M_{Z_s}} \right)^2 \right] \\ &+ \frac{g_2^2 m_\mu^2}{8\pi^2 M_Z^2 c_W^2} \left[\left(s_W^2 - \frac{1}{3} \right) s_\eta c_\eta s_W s_\epsilon + \frac{1}{6} s_W^2 s_\epsilon^2 s_\eta^2 \right] \\ &- \frac{g_2^2 m_\mu^2}{8\pi^2 M_{Z_s}^2 c_W^2} \left[\left(s_W^2 - \frac{1}{3} \right) s_\eta c_\eta s_W s_\epsilon - \frac{1}{6} s_W^2 s_\epsilon^2 s_\eta^2 \right] \\ &= 1.94 \times 10^{-9} \left(1 - \frac{M_Z^2}{M_{Z_s}^2} \right) \\ &\times [s_\eta^2 - 0.2354 s_\eta c_\eta s_\epsilon + 0.1850 s_\epsilon^2 s_\eta^2], \quad (26) \end{aligned}$$

where we have set $s_W^2 = 0.2311$. The W boson and other SM contributions remain the same. The two Higgs

bosons and higher loop diagrams contribute negligibly. We shall see later that δa_μ above does not give better constraints than EWPT.

B. NuTeV

The NuTeV experiment measures the ratio of neutral current to charged current cross-sections in deep-inelastic ν_μ -nucleon scattering [9]. As was suggested by Paschos-Wolfenstein [10] to reduce theoretical and systematic uncertainties, the precision observable to measure at NuTeV is

$$\begin{aligned} R_{PW} &= \frac{\sigma(\nu_\mu N \rightarrow \nu_\mu X) - \sigma(\bar{\nu}_\mu N \rightarrow \bar{\nu}_\mu X)}{\sigma(\nu_\mu N \rightarrow \mu X) - \sigma(\bar{\nu}_\mu N \rightarrow \mu^+ X)} \\ &= (g_L^N)^2 - (g_R^N)^2 = \frac{1}{2} - s_W^2, \end{aligned} \quad (27)$$

where $(g_{L,R}^N)^2 = (g_{L,R}^u)^2 + (g_{L,R}^d)^2$. Since the shadow world affects only the neutral current processes, presence of a new neutral gauge boson will only affect the numerator of R_{PW} . For the $\nu_\mu q$ elastic scattering process, the squared amplitude receives corrections from the modifications in the couplings of the SM Z , and from contributions due to the exchange of the virtual Z_s . Incorporating these effects due to the Z_s , a straightforward calculation shows that the numerator of R_{PW} is proportional to

$$\begin{aligned} \sum_{q=u,d} \left\{ \left[(g_L^q)^2 - (g_R^q)^2 \right] + 2 \frac{M_Z^2}{M_{Z_s}^2} g_L^q [x_L^q g_L^q - x_R^q g_R^q] \right\} \\ + \mathcal{O} \left(\frac{M_Z^4}{M_{Z_s}^4} \right), \end{aligned} \quad (28)$$

where $x_{L,R}^f = -(s_\eta g_{L,R}^f + c_\eta Y^f s_W s_\epsilon)$ is the $Z_s f \bar{f}$ coupling given in Eq.(12), and $q^2 \ll M_Z^2, M_{Z_s}^2$ is assumed, with q the momentum transfer. The first term in Eq. (28) is the SM result, while the second term comes from the SM-shadow interference; we have ignored the term suppressed by $(M_Z/M_{Z_s})^4$. Note that for the isoscalar targets considered at NuTeV, the sum is over u and d quark distributions. Assuming that $M_{Z_s} \gg M_Z$, only the SM contribution need be kept while taking into account the modifications to the Z -fermion coupling. In terms of the mixing parameters of our model, the effective nucleon coupling to the SM Z is given by:

$$\begin{aligned} (g_L^N)^2 &\simeq (g_L^N)_{SM}^2 [1 - 2s_\eta^2 + 1.0028s_\eta c_\eta s_\epsilon], \\ (g_R^N)^2 &\simeq (g_R^N)_{SM}^2 [1 - 2s_\eta^2 + 5.1218s_\eta c_\eta s_\epsilon]. \end{aligned} \quad (29)$$

Note that the coupling to neutrinos is absorbed into the effective couplings here.

C. Møller Scattering at SLAC

The SLAC E158 Møller scattering experiment [11] measures the parity violating asymmetry,

$$A_{PV} = \frac{\sigma_L - \sigma_R}{\sigma_L + \sigma_R}, \quad (30)$$

at momentum transfer $Q^2 = 0.026 \text{ GeV}^2$. The subscripts L and R denote the incident electron polarization. At tree level, the asymmetry is, up to $\mathcal{O}(g_2^2)$:

$$A_{PV} \simeq \frac{G_F s}{\sqrt{2}\pi\alpha} \frac{y(1-y)}{1+y^4+(1-y)^4} (g_L^{e2} - g_R^{e2}), \quad (31)$$

where $y = Q^2/s \simeq 0.6$.

The denominator in the above expression represent the leading Møller cross-section due to photon exchange, and the numerator is the parity violation due to photon- Z interference. It is easy to extend it to include the Z_s contribution. We only need to keep the photon- Z_s interference term:

$$A_{PV}^{Z_s} \simeq \frac{G_F s}{\sqrt{2}\pi\alpha} \frac{y(1-y)}{1+y^4+(1-y)^4} (x_L^{e2} - x_R^{e2}) \left(\frac{M_Z}{M_{Z_s}} \right)^2 \quad (32)$$

Assuming that $M_{Z_s} \gg M_Z$, the Z_s effect can be ignored. From the modified $Z e \bar{e}$ coupling we have

$$\begin{aligned} \frac{\delta A_{PV}}{A_{PV}} &\simeq -s_\eta^2 - \frac{3}{4} \frac{s_\eta^2 s_W^2 s_\epsilon^2}{\frac{1}{4} - s_W^2} - c_\eta s_\eta s_W s_\epsilon \frac{s_W^2 + \frac{1}{2}}{\frac{1}{4} - s_W^2} \\ &\simeq -[s_\eta^2 + 9.171s_\eta^2 s_\epsilon^2 + 18.60c_\eta s_\eta s_\epsilon]. \end{aligned} \quad (33)$$

This translates into

$$\begin{aligned} \delta \sin^2 \theta_{eff} &\simeq -\frac{1 - 4s_W^2}{4} \frac{\delta A_{PV}}{A_{PV}} \\ &\simeq 0.019 [s_\eta^2 + 9.17s_\eta^2 s_\epsilon^2 + 18.60c_\eta s_\eta s_\epsilon] \end{aligned} \quad (35)$$

D. Atomic Parity Violation

In the atomic system, the exchange of SM Z boson will generate the parity violating $M1$ transition. This optical line can be accurately measured and used to compare with the theoretical prediction [12]. Since the momentum transferred by the Z boson is much smaller than nuclear mass, it can sense the weak charge of all the quarks coherently. The relevant quantity is:

$$\begin{aligned} Q_W &= -4(g_L^e - g_R^e)[(2Z + N)(g_L^u + g_R^u) \\ &\quad + (2N + Z)(g_L^d + g_R^d)]. \end{aligned} \quad (36)$$

The expression for the contribution from an extra neutral gauge boson, X , is same as above with $g_{L,R}$ changed to the corresponding couplings for X and multiplied by an extra mass factor m_Z^2/m_X^2 .

If Z_s is much heavier than the SM Z , its tree-level effect goes like $s_\epsilon^2(M_Z/M_{Z_s})^2$, which can be again ignored.

Therefore, the leading change to Q_W comes from the modification to the couplings of SM Z boson to fermions. At tree level, we have for C_s^{133}

$$\frac{\delta Q_W}{Q_W} \simeq -s_\eta^2 + 0.7605s_\eta^2s_\epsilon^2 + 2.0627c_\eta s_\eta s_\epsilon, \quad (37)$$

and for Tl_{81}^{205}

$$\frac{\delta Q_W}{Q_W} \simeq -s_\eta^2 + 0.7195s_\eta^2s_\epsilon^2 + 1.9774c_\eta s_\eta s_\epsilon. \quad (38)$$

E. Asymmetries at LEP

Consider first the general expression of differential cross section for the process $e^- + e^+ \rightarrow f^- + f^+$ mediated by more than one neutral gauge boson. If we ignored all the light fermion masses, the differential cross section for f^- deflected from the incident e^- direction by angle θ are given by:

$$\begin{aligned} \frac{d\sigma}{d(\cos\theta)} = \frac{N_c\pi\alpha^2}{8s} \sum_{X,Y} K_{XY} \left\{ (1 + \cos\theta)^2 \left(g_{XL}^e g_{YL}^e g_{XL}^f g_{YL}^f + g_{XR}^e g_{YR}^e g_{XR}^f g_{YR}^f \right) \right. \\ \left. + (1 - \cos\theta)^2 \left(g_{XL}^e g_{YL}^e g_{XR}^f g_{YR}^f + g_{XR}^e g_{YR}^e g_{XL}^f g_{YL}^f \right) \right\}, \end{aligned} \quad (39)$$

where indices X, Y run over all neutral gauge bosons and the K 's are kinematic factors. For instance, $K_{\gamma\gamma} = Q_f^2$, and for $X, Y \neq \gamma$,

$$K_{X\gamma} = \left(\frac{-2Q_f}{c_W^2 s_W^2} \right) \frac{s(s - M_X^2)}{[(s - M_X^2)^2 + M_X^2 \Gamma_X^2]}, \quad (40)$$

$$K_{XX} = \left(\frac{1}{c_W^4 s_W^4} \right) \frac{s^2}{(s - M_X^2)^2 + M_X^2 \Gamma_X^2}, \quad (41)$$

$$K_{XY} = \left(\frac{2}{c_W^4 s_W^4} \right) \frac{s^2[(s - M_Y^2)(s - M_X^2) + M_Y \Gamma_Y M_X \Gamma_X]}{[(s - M_Y^2)^2 + M_Y^2 \Gamma_Y^2][(s - M_X^2)^2 + M_X^2 \Gamma_X^2]}, \quad (42)$$

where M and Γ are the mass and width of the neutral gauge boson respectively. For photon coupling, it has been normalized to be $g_L = g_R = 1$. For other neutral gauge boson coupling, the coupling is normalized by the SM strength (g_2/c_W). The forward-backward asymmetry is then given by

$$A_{FB}^f = \frac{3}{4} \frac{\sum_{X,Y} K_{XY} (g_{XL}^e g_{YL}^e - g_{XR}^e g_{YR}^e) (g_{XL}^f g_{YL}^f - g_{XR}^f g_{YR}^f)}{\sum_{X,Y} K_{XY} (g_{XL}^e g_{YL}^e + g_{XR}^e g_{YR}^e) (g_{XL}^f g_{YL}^f + g_{XR}^f g_{YR}^f)}. \quad (43)$$

In SM, the fermion's left-right asymmetry can be derived from the left-right forward-backward asymmetry:

$$A_f = \frac{4}{3} \frac{\sigma_{LF}^f - \sigma_{LB}^f - \sigma_{RF}^f + \sigma_{RB}^f}{\sigma_{LF}^f + \sigma_{LB}^f + \sigma_{RF}^f + \sigma_{RB}^f}, \quad (44)$$

where L (R) stands for the left(right)-handed incident electron, and F (B) stands for the forward (backward) direction, $\cos\theta > 0$ (< 0), of the final state fermion. When more than one massive neutral gauge bosons are present, the effective left-right asymmetry becomes:

$$A_f = \frac{\sum_{X,Y} K_{XY} (g_{XL}^e g_{YL}^e + g_{XR}^e g_{YR}^e) (g_{XL}^f g_{YL}^f - g_{XR}^f g_{YR}^f)}{\sum_{X,Y} K_{XY} (g_{XL}^e g_{YL}^e + g_{XR}^e g_{YR}^e) (g_{XL}^f g_{YL}^f + g_{XR}^f g_{YR}^f)}. \quad (45)$$

At the Z pole, $K_{ZZ} = 42298.1$. The other K factors are very small and all of them can be ignored except K_{XX} , which has a very narrow and high spike when $M_{Z_s} \sim M_Z$. However, it drops very quickly when M_{Z_s} fall outside the Z width. Therefore, for a heavy Z_s we only need to

consider the modification of the SM $Zf\bar{f}$ coupling and its effect on the precision measurement.

In Table I, we summarize the current LEP, NuTeV, and SLAC Møller status (from [13]) and our prediction. The second column Δ_{exp} is the experimental fractional

deviation from the SM prediction and the combined theoretical and experimental uncertainty, (δ_{exp}), is shown in the parenthesis. The third column gives the fractional deviation from the SM our shadow model predicts.

| Quantity | $\Delta_{exp} \equiv \left(\frac{\text{Exp}}{\text{SM}}\right) - 1$ | $\Delta_s \equiv \left(\frac{\text{Model}}{\text{SM}}\right) - 1$ |
|-----------------------|---|---|
| Γ_Z | -0.0008(10) | $-s_\eta^2 + 0.5730s_\eta c_\eta s_\epsilon$ |
| σ_{had} | +0.0017(9) | $+0.02593s_\eta c_\eta s_\epsilon$ |
| $\Gamma(had)$ | +0.0005(13) | $-s_\eta^2 + 0.4327s_\eta c_\eta s_\epsilon$ |
| $\Gamma(inv)$ | -0.0056(30) | $-s_\eta^2 + 0.961s_\eta c_\eta s_\epsilon$ |
| $\Gamma(l\bar{l})$ | -0.00048(107) | $-s_\eta^2 + 0.7393s_\eta c_\eta s_\epsilon$ |
| R_e | +0.0026(25) | $-0.3065s_\eta c_\eta s_\epsilon$ |
| R_μ | +0.0016(17) | $-0.3065s_\eta c_\eta s_\epsilon$ |
| R_τ | -0.0013(23) | $-0.3065s_\eta c_\eta s_\epsilon$ |
| R_b | +0.0034(31) | $+0.0676s_\eta c_\eta s_\epsilon$ |
| R_c | -0.0019(174) | $-0.1306s_\eta c_\eta s_\epsilon$ |
| $A_{FB}^{(0,e)}$ | -0.108(154) | $-38.67s_\eta c_\eta s_\epsilon$ |
| $A_{FB}^{(0,\mu)}$ | +0.039(82) | $-38.67s_\eta c_\eta s_\epsilon$ |
| $A_{FB}^{(0,\tau)}$ | +0.156(106) | $-38.67s_\eta c_\eta s_\epsilon$ |
| $A_{FB}^{(0,b)}$ | -0.034(17) | $-19.59s_\eta c_\eta s_\epsilon$ |
| $A_{FB}^{(0,c)}$ | -0.043(48) | $-21.24s_\eta c_\eta s_\epsilon$ |
| $A_{FB}^{(0,s)}$ | -0.055(111) | $-19.59s_\eta c_\eta s_\epsilon$ |
| A_e | +0.028(16) | $-19.335s_\eta c_\eta s_\epsilon$ |
| | +0.049(42) | $-19.335s_\eta c_\eta s_\epsilon$ |
| | +0.018(34) | $-19.335s_\eta c_\eta s_\epsilon$ |
| A_μ | -0.035(102) | $-19.335s_\eta c_\eta s_\epsilon$ |
| A_τ | -0.076(102) | $-19.335s_\eta c_\eta s_\epsilon$ |
| | -0.022(30) | $-19.335s_\eta c_\eta s_\epsilon$ |
| A_b | -0.010(21) | $-0.251s_\eta c_\eta s_\epsilon$ |
| A_c | +0.003(39) | $-1.909s_\eta c_\eta s_\epsilon$ |
| A_s | -0.043(97) | $-0.251s_\eta c_\eta s_\epsilon$ |
| <hr/> | | |
| NuTeV | | |
| $(g_L^N)^2$ | -0.013(5) | $-2s_\eta^2 + 1.0028s_\eta c_\eta s_\epsilon$ |
| $(g_R^N)^2$ | +0.023(36) | $-2s_\eta^2 + 5.1218s_\eta c_\eta s_\epsilon$ |
| <hr/> | | |
| SLAC Møller | | |
| $\sin^2 \theta_{eff}$ | +0.007(22) | $0.019s_\eta^2 + 0.353s_\eta c_\eta s_\epsilon$ |
| $Q_W(Cs^{133})$ | -0.0068(66) | $-s_\eta^2 + 2.0627c_\eta s_\eta s_\epsilon$ |
| $Q_W(Tl^{205})$ | -0.0018(317) | $-s_\eta^2 + 1.9774c_\eta s_\eta s_\epsilon$ |

TABLE I: The comparison of experimental values and theoretical prediction, up to $\mathcal{O}(s_\epsilon^2)$, for various EWPT observables.

To give a measure of how well our model fits the data from EWPTs compare to that using purely the SM, we define a number, χ_2 , that measures the deviation between theory and experiment,

$$\chi_2(s_\epsilon, M_3) \equiv \sum_i \left(\frac{\Delta_{exp}^i - \Delta_s^i}{\delta_{exp}^i} \right)^2. \quad (46)$$

For SM only, the deviation is

$$\chi_2^{SM} = \chi_2(0, M_3) = \chi_2(s_\epsilon, \infty) = 34.908. \quad (47)$$

The parameter space allowed for s_ϵ and M_3 (or s_η) will be determined by doing a simple least square fit. We are interested in getting a solution which can lower the χ_2 , or

$$\Delta\chi_2 \equiv \chi_2(s_\epsilon, M_3) - \chi_2^{SM} \leq 0, \quad (48)$$

indicating a better fit than the SM. However, for $M_3 > 200$ GeV, our numerical search did not find any parameter space which can improve the global fitting listed in Table I. This is easy to understand. For $M_{Z_s} \gg M_Z$, $s_\eta \ll s_\epsilon$ and the s_η^2 corrections in the third column of the table is not important. One sees that about half of the EW observables get the wrong sign corrections. Therefore at most we can only make gain and loss balanced.

Therefore, we demand that the allowed parameter space does not make the fitting worse and this is shown as the lower band in Fig. 2. The allowed parameter region

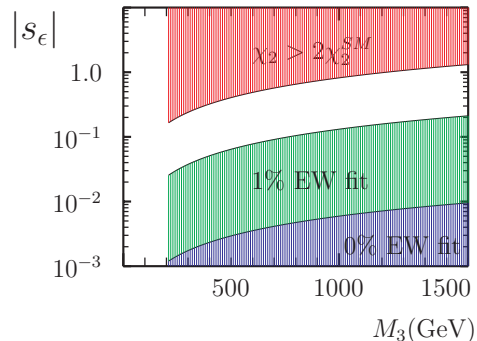


FIG. 2: The bound on s_ϵ and M_3 from EWPT. The upper band is the excluding region by too large a deviation from SM, $\chi_2 > 2\chi_2^{SM}$. The lower band in the parameter space gives comparable to SM results in the global fit. And the middle one is the allowed region where $(\Delta\chi_2/\chi_2^{SM}) < 0.01$.

is approximately given by

$$M_3 > 166|s_\epsilon| \text{ TeV} \quad \text{or} \quad |s_\epsilon| < 0.006 \left(\frac{M_3}{1 \text{ TeV}} \right). \quad (49)$$

However, if we relax the global fitting a little, $(\Delta\chi_2/\chi_2^{SM}) < 0.01$, the constraint can be much looser (see the middle band in Fig. 2). Hereafter, the ceiling boundaries of the middle and lower bands will be referred as 1%EWPT and 0%EWPT respectively.

IV. THE LHC AND THE ILC

Here we calculate the Z_s Drell-Yan processes at the LHC given the constraints on its couplings obtained above. One needs to fold in the parton distributions of $u(d)$ and $\bar{u}(\bar{d})$ inside the proton. This involves QCD corrections to the parton model, and are extensively studied with relatively good theoretical control [14]. It is also very well tested for the Z production at the Tevatron.

Assume narrow width approximation,

$$\frac{q^4}{|q^2 - M_{Z_s}^2 + iM_{Z_s}\Gamma_{Z_s}|^2} \rightarrow \delta(q^2 - M_{Z_s}^2) \frac{\pi M_{Z_s}^4}{M_{Z_s}\Gamma_{Z_s}}, \quad (50)$$

the expected number of observed events, say by reconstructing from the $\mu^+\mu^-X$ final states, is

$$\begin{aligned} N_{Z_s} &= L\sigma_T(pp \rightarrow Z_s X \rightarrow \mu^+\mu^-X) \\ &\simeq \frac{L}{s} C_{Z_s} C \exp\left[-A \frac{M_{Z_s}}{\sqrt{s}}\right], \end{aligned} \quad (51)$$

where

$$\begin{aligned} C_{Z_s}(Z_s \rightarrow \mu^+\mu^-) &= \frac{4\pi^2}{3} \frac{\Gamma(Z_s)}{M_{Z_s}} Br(Z_s \rightarrow \mu^+\mu^-) \\ &\times \left[Br(Z_s \rightarrow u\bar{u}) + \frac{1}{C_{ud}} Br(Z_s \rightarrow d\bar{d}) \right], \end{aligned} \quad (52)$$

L is the luminosity, C_{ud} is the ratio of u(d)-parton distribution inside the proton. For the pp hadron collider, $C_{ud}(pp) \sim 2$, $A(pp) \sim 32$, and $C(pp) \sim 600$ for a very wide range of s [14].

In order to select a signal, it is essential to know the branching ratios of Z_s . The calculation for Z_s decays into fermion pair is straightforward. For the SM fermions, they are (again setting $s_W^2 = 0.2311$):

$$\begin{aligned} \Gamma(Z_s \rightarrow u\bar{u}) &= \frac{1}{24\pi} \frac{g_2^2}{c_W^2} M_{Z_s} [0.32739s_\epsilon^2(1 - s_\eta^2) \\ &\quad - 0.129957s_\eta c_\eta s_\epsilon + 0.43022s_\eta^2], \end{aligned} \quad (53)$$

$$\begin{aligned} \Gamma(Z_s \rightarrow d\bar{d}) &= \frac{1}{24\pi} \frac{g_2^2}{c_W^2} M_{Z_s} [0.09629s_\epsilon^2(1 - s_\eta^2) \\ &\quad - 0.277396s_\eta c_\eta s_\epsilon + 0.55451s_\eta^2], \end{aligned} \quad (54)$$

$$\begin{aligned} \Gamma(Z_s \rightarrow e\bar{e}) &= \frac{1}{24\pi} \frac{g_2^2}{c_W^2} M_{Z_s} [0.28888s_\epsilon^2(1 - s_\eta^2) \\ &\quad - 0.09293s_\eta c_\eta s_\epsilon + 0.12571s_\eta^2], \end{aligned} \quad (55)$$

$$\begin{aligned} \Gamma(Z_s \rightarrow \nu\bar{\nu}) &= \frac{1}{24\pi} \frac{g_2^2}{c_W^2} M_{Z_s} [0.05777s_\epsilon^2(1 - s_\eta^2) \\ &\quad - 0.240364s_\eta c_\eta s_\epsilon + 0.25s_\eta^2]. \end{aligned} \quad (56)$$

After crossing the $t\bar{t}$ threshold, Z_s can decay into a pair of t-quarks. We find

$$\frac{\Gamma(Z_s \rightarrow t\bar{t})}{\Gamma(Z_s \rightarrow u\bar{u})} = \sqrt{1 - 4\beta} [1 + 0.41176\beta + 0.7979\beta^2] \quad (57)$$

where $\beta = (M_t/M_{Z_s})^2$ and the β^2 term comes from the expansion of s_η/s_ϵ . The decay into a W^+W^- pair has width

$$\begin{aligned} \Gamma(Z_s \rightarrow W^+W^-) &= \frac{g_2^2 c_W^2 s_\eta^2}{192\pi} \frac{M_{Z_s}^5}{M_W^4} (1 - 4y)^{3/2} \\ &\times (1 + 20y + 12y^2), \quad y = \frac{M_W^2}{M_{Z_s}^2}. \end{aligned} \quad (58)$$

If M_{Z_s} is heavier than $(M_Z + M_{h_1^0})$, and the kinematics are favorable, there is a new decay channel opening up,

$$\begin{aligned} \Gamma(Z_s \rightarrow Zh_1^0) &\simeq \frac{g_2^2 c_\alpha^2}{192\pi c_W^2} (c_\eta + s_W s_\epsilon s_\eta)^2 (s_\eta - s_W s_\epsilon c_\eta)^2 \\ &\times M_{Z_s} \sqrt{1 - 4z} (1 + 8z), \quad z = \frac{M_Z^2}{M_{Z_s}^2}, \end{aligned} \quad (59)$$

where we have ignored the mass difference between h_1^0 and Z to simplify the expression. The branching ratio of shadow Z as a function of its mass is displayed in Fig. 3. In generating the figure we have treated M_{Z_s} and s_ϵ as

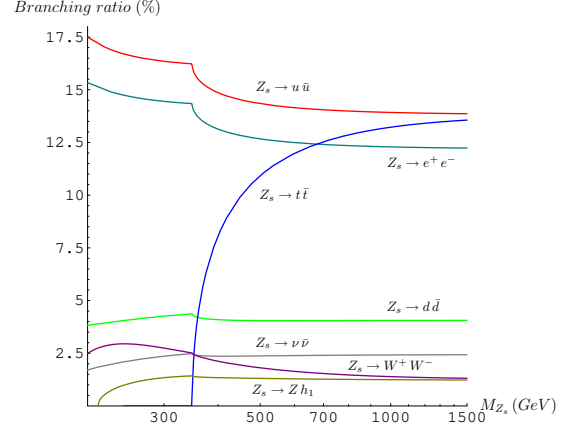


FIG. 3: Branching ratio for the Z_s decays as functions of M_{Z_s} . The curves shown here are generated with $M_{h_1^0} = 120$ GeV and c_α , the Higgs mixing angle as defined in Eq. (17), set to one.

independent parameters and used a very small value of $s_\epsilon = 10^{-3}$. This is consistent with the bound of Fig. 2.

In the large M_{Z_s} limit, say > 1.0 TeV, the s_ϵ^2 -terms will dominate and we obtain a very simple expression for the decay width:

$$\Gamma_{Z_s} \simeq 2.37 \frac{g_2^2 M_{Z_s} s_\epsilon^2}{24\pi c_W^2} = 0.1742 \left(\frac{M_{Z_s}}{1 \text{ TeV}} \right) \left(\frac{s_\epsilon^2}{0.01} \right) \text{ GeV}. \quad (60)$$

We see that for such a heavy Z_s its width is indeed very narrow, and the various branching ratios are approximately given by

$$\begin{aligned} B_u &= B_c = B_t \simeq 13.81\%, \\ B_d &= B_s = B_b \simeq 4.06\%, \\ B_e &= B_\mu = B_\tau \simeq 12.19\%, \\ B_{\nu_e} &= B_{\nu_\mu} = B_{\nu_\tau} \simeq 2.44\%, \\ B_{W^+W^-} &\simeq 1.219\%, \\ B_{Zh_1^0} &\simeq 1.219c_\alpha^2\%. \end{aligned} \quad (61)$$

For SM fermions, the branching ratio is roughly proportional to $(Y_L^2 + Y_R^2)$. It's interesting to note that Z_s prefers to decay into u -type quarks and charged leptons than other SM fermions. This is very different from the SM Z

decay. If the ILC is available, and the Z_s is found, this unique prediction may be tested.

At the LHC with the center of mass energy $\sqrt{s} = 14$ TeV and using the bench mark luminosity of $L = 100 \text{ fb}^{-1}$, we calculated the expected number of events of Z_s into different decay modes by simply folding in the branching ratio we obtained earlier and taking into account of the phase space factors.

More importantly, one has to carefully take into account the maximally allowed s_ϵ obtained from the global fit of low energy precision measurements as given previously. The expected number of events depend on how restricted we are in taking the EWPTs. Fig. 4 shows the sensitivity to the $\Delta\chi_2/\chi_2^{SM}$ which can lead to two

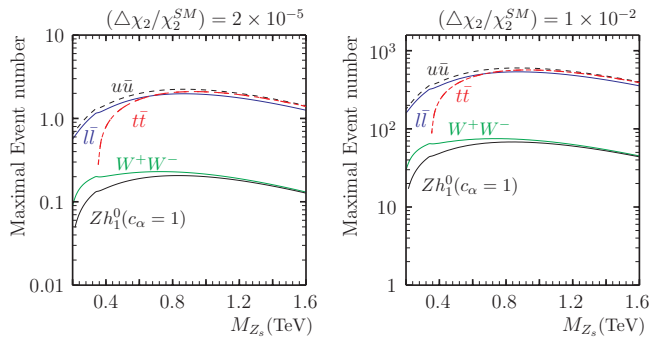


FIG. 4: The maximal expected number of Z_s events at the LHC for integrated luminosity of 100 fb^{-1} . For a fixed M_{Z_s} , we have used the largest allowed s_ϵ comes from the global fit studied in previous section. The left and right panes are for 0%EWPT and 0%EWPT respectively.

orders of magnitude difference in the signature. Notice the dipping of the signals for smaller M_{Z_s} . This is due to the much smaller values of s_ϵ allowed for these relatively light Z_s .

One way of distinguishing between different extra Z models will be measuring the branching ratios into different fermion species. The Z_s has the feature that it has a relatively large branching ratio into charged leptons and the t-quarks. For sufficiently heavy Z_s the two branching ratios are almost equal. Whether this can be used as a diagnostic tool at the LHC depends on the t-jets and c-jets efficiencies.

The success of LEP has demonstrated that e^+e^- colliders are powerful machines for studying neutral gauge bosons. Indeed the search of extra Z bosons has been conducted at LEP and the results can be found in reference [15]. Looking forward to the ILC, the center of mass energy of the collider is lower than that of the LHC with $\sqrt{s} = 1$ TeV. We can still expect to see extra Z 's of mass below 1 TeV to be produced. On the other hand, facilities designed to have higher luminosity and a benchmark integrated luminosity of 500 fb^{-1} can be expected. Furthermore, the underlying processes involve much less QCD uncertainties than in hadronic machines, making it a cleaner environment for detecting the extra Z bosons. Thus, we can anticipate the branching ratios to be ac-

curately measured. Moreover, the Z_s will be too narrow for the total width to be measured. However, spikes will be seen at the mass where LHC “discovered” the new state. In Fig. 5 we display the result of such a hypothetical occurrence of a Z_s of mass $M_{Z_s} = 500$ GeV and $s_\epsilon = 0.066$ corresponding to the maximal allowed value from the 1%EWPT fit. The familiar SM Z boson resonance peaks sit on the left hand side. A new spike appears at M_{Z_s} . We magnify the event shape around $\sqrt{s} = 0.5$ TeV and we see the characteristic dip at the left base of the peak corresponding to an extra Z . This dip is due to the negative contribution from $\gamma - Z_s$ and $Z-Z_s$ interference. Although the resonance factor $K_{Z_s Z_s}$ dominates over $K_{Z_s \gamma}$, $K_{Z_s Z}$ around M_{Z_s} , the $K_{Z_s Z_s}$ gets an extra s_ϵ^2 suppression in couplings compared to $K_{Z_s \gamma}$ and $K_{Z_s Z}$ which makes the dip visible.

For 0%EWPT fit, not shown, the spike is not as pronounced and the width is thinner, thus its studies at the ILC will be more challenging. Similarly, the ratio

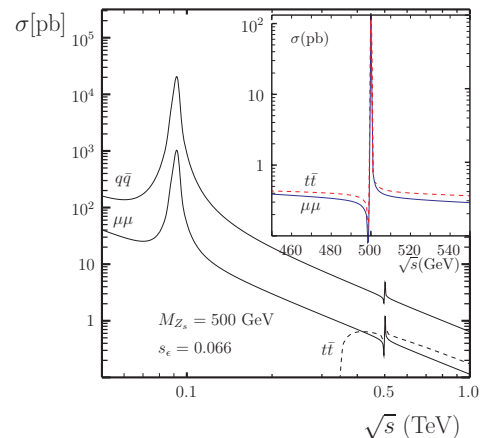


FIG. 5: The cross section for $e^+e^- \rightarrow f\bar{f}$ with a 500 GeV Z_s and $s_\epsilon = 0.066$. (In the main frame, the spike tips have been chopped to avoid overlapping among curves.)

$$R^{had} = \frac{Br(e^+e^- \rightarrow q\bar{q})}{Br(e^+e^- \rightarrow \mu^+\mu^-)}, \quad (62)$$

where q sums over all quarks except the top, has a pronounced spike for 1%EWPT fit. This is shown in Fig. 6. The inlay magnifies the region around Z_s and illustrates the expected interference pattern of two spin-1 particles is clearly discernible. The unique event shape is characteristic of this model which may be used to discriminate it from other extra Z models. Finally, the forward-backward asymmetry of muon v.s. \sqrt{s} is shown in Fig. 7.

V. CONCLUSIONS

We have studied in detail a simple model with an extra neutral $U(1)$ boson, dubbed shadow Z . The shadow Z

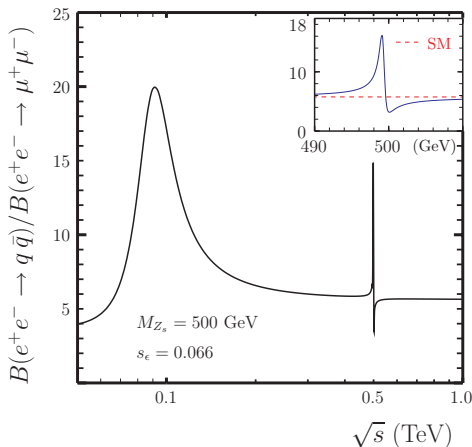


FIG. 6: The ratio of $e^+e^- \rightarrow \sum_{q \neq t} q\bar{q}$ over $e^+e^- \rightarrow \mu^+\mu^-$ with a 500 GeV Z_s and $s_\epsilon = 0.066$.

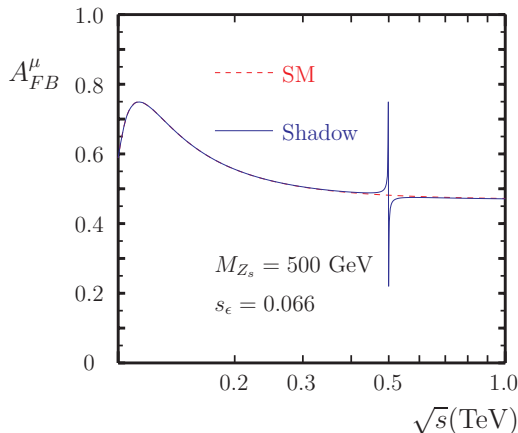


FIG. 7: The forward-backward asymmetry of muon v.s. \sqrt{s} with a 500 GeV Z_s and $s_\epsilon = 0.066$.

mixes with the SM $U(1)_Y$ gauge boson kinetically which is parameterized by s_ϵ . The Higgs sector also contains a scalar field that interacts with the SM Higgs field. There is no direct coupling between the shadow Z and the SM fermions. This simple model can easily be embedded in more elaborate model. Since our motivation is purely phenomenological we leave this aspect to a future study. Instead we embark on a detail analysis of the EWPT constraints and other low energy precision measurements on M_{Z_s} and s_ϵ . It is well known that s_ϵ can vary greatly from model to model. We found that the data constrain

it to be very small for a wide range of extra Z boson masses; see Eq. (49). We conclude that the data favors those models in which s_ϵ is radiatively generated.

Not surprisingly the production of Z_s at the LHC and the ILC depends crucially on s_ϵ . In order to ascertain whether the signals are observable we define a figure of merit measure given by $\Delta\chi_2$ (see Eq. (48)) which we found to be positive. We conclude that the shadow Z does not give a better global fit to the EWPTs. However, we use $\Delta\chi_2$ to quantify the data tolerance to Z_s . We found that $(\Delta\chi_2/\chi_2^{SM}) \sim 0.01$ will lead to an observable production of Z_s via the Drell-Yan process at the LHC.

To distinguish the shadow Z from other extra Z models (see [7]) one has to do as many branching ratio measurements as possible. The shadow Z has almost equal branching ratios into u-type quarks and charged leptons. It also has a decay channel into the SM like Z and Higgs boson although it is only 1.3%. Similarly for the decay into W^+W^- pairs. For this we find that the ILC will be invaluable for pinning down the nature of the extra Z boson.

Acknowledgments

The research of W.F.C. is supported by the Academia Sinica Postdoctoral Fellowship, Taiwan. W.F.C. would like to thank the TRIUMF theory group for their kind hospitality where part of this work is done. J.N.N would like to thank Prof. R. Casalbuoni for providing a warm and stimulating environment at the GGI, Florence, where the early part of this work was done. He also gratefully acknowledge the efforts of Prof. B. Vachon of keeping him informed of the experimental situation in extra Z searches. The authors would like to thank Prof. B. Holdom for useful comments. This research is partially supported by the Natural Science and Engineering Council of Canada.

Note Added

After the completion of this paper our attention was drawn to an earlier work that had looked at similar Z' models [16], and also the Stueckelberg Z' model which has almost identical collider signatures [17] and a similar electroweak fit [18]. We have checked that our results agree where they overlap. A variant of the model has also been used in a recent leptogenesis study [19].

- [1] see, e.g. R. W. Robinett and J. L. Rosner, Phys. Rev. D **25**, 3036 (1982), D **27**, 679 (1983) (E); P. Langacker, R. W. Robinett and J. L. Rosner, Phys. Rev. D **30**, 1470 (1984); F. Zwirner, Int. J. Mod. Phys. A **3**, 49 (1988).
 [2] B. Holdom, Phys. Lett. B **166**, 196 (1986), B **259**, 329 (1991).

- [3] K. S. Babu, C. F. Kolda and J. March-Russell, Phys. Rev. D **54**, 4635 (1996), hep-ph/9603212; K. S. Babu, C. F. Kolda and J. March-Russell, Phys. Rev. D **57**, 6788 (1998), hep-ph/9710441.
 [4] K.R. Dienes, C. Kolda, and J. March-Russell, Nucl. Phys **492**, 104 (1997)

- [5] J. Kumar and J. D. Wells, hep-ph/0606183.
- [6] J. L. Hewett and T. G. Rizzo, Phys. Rept. **183**, 193 (1989).
- [7] A. Leike, Phys. Rept. **317**, 143 (1999), hep-ph/9805494.
- [8] B. Patt and F. Wilczek, hep-ph/0605188.
- [9] G. P. Zeller *et al.* [NuTeV Collaboration], Phys. Rev. Lett. **88**, 091802 (2002), **90**, 239902 (2003) (**E**), hep-ex/0110059.
- [10] E. A. Paschos and L. Wolfenstein, Phys. Rev. D **7**, 91 (1973).
- [11] P. L. Anthony *et al.* [SLAC E158 Collaboration], Phys. Rev. Lett. **95**, 081601 (2005), hep-ex/0504049.
- [12] P. A. Vetter, D. M. Meekhof, P. K. Majumder, S. K. Lamoreaux and E. N. Fortson, Phys. Rev. Lett. **74**, 2658 (1995); S. C. Bennett and C. E. Wieman, Phys. Rev. Lett. **82**, 2484 (1999), hep-ex/9903022.
- [13] S. Eidelman *et al.* [Particle Data Group], Phys. Lett. B **592**, 1 (2004).
- [14] A. Leike, Phys. Lett. B **402**, 374 (1997), hep-ph/9703263.
- [15] [LEP Collaboration], hep-ex/0312023.
- [16] T. Appelquist, B. A. Dobrescu and A. R. Hopper, Phys. Rev. D **68**, 035012 (2003)
- [17] B. Kors and P. Nath, Phys. Lett. B **586**, 366 (2004); B. Kors and P. Nath, JHEP **0507**, 069 (2005); D. Feldman, Z. Liu and P. Nath, arXiv:hep-ph/0606294.
- [18] D. Feldman, Z. Liu and P. Nath, Phys. Rev. Lett. **97**, 021801 (2006).
- [19] D. G. Cerdeno, A. Dedes and T. E. J. Underwood, hep-ph/0607157.